Plasmon decay mechanisms in proton-solid collisions

G. A. Bocan and J. E. Miraglia
Instituto de Astronomía y Física del Espacio, Consejo Nacional de Investigaciones Científicas y Técnicas, Departamento de Física, Facultad de Ciencias Exactas y Naturales, Universidad de Buenos Aires, Casillo de Correo 67, Sucursal 28, 1428 Buenos Aires, Argentina
(Received 15 June 2005; published 28 October 2005)

A projectile traveling inside a metal can excite bulk plasmons (collective oscillations of the electron gas) that eventually decay. The two main decay mechanisms are the excitation of a nearly free electron (NFe), also referred to as a Bloch electron, and the excitation of a pair of interacting free electrons ($2e$). In recent publications we developed a model to study these mechanisms for proton impact on aluminum. In this paper, we apply that model to other simple metals. Interesting results are obtained for magnesium, sodium, and potassium. The comparison of the NFe energy and angular spectra sheds light on the role the crystal structure plays. Results for the total probability and excitation power can also be understood in terms of the elements' different characteristics. Some comments are made regarding the relative importance of the two mechanisms for each element and the role that parameters like the electron density, the crystal structure, and the plasmon linewidth might play in this. Also, an approximate scaling rule is found for the plasmon creation probability as well as for the $2e$ contribution to the plasmon decay probability.

DOI: 10.1103/PhysRevA.72.042903 PACS number(s): 79.20.Ap, 34.10.+x

I. INTRODUCTION

The excitation of collective modes (plasmons) in a degenerate electron gas is well established in both theory and experiment. It is also common knowledge that those plasmons cannot transfer their energy and momentum to a single free electron. In order for the plasmon to decay, the electron to be excited needs a partner.

Different authors have suggested and studied possible plasmon excitation and decay mechanisms. Experimental results present evidence of plasmon excitation for both fast [1–7] and slow [8–12] ions in grazing incidence on metallic surfaces. These plasmons decay, transferring their energy and momentum to electrons that are emitted in a very specific energy range.

The most important plasmon decay mechanisms mentioned in the literature are the excitation of a Bloch electron (that undergoes an interband transition) [13–16] and the excitation of a pair of free interacting electrons [17]. In two recent papers [18,19], henceforth referred to as I and II, we developed a formalism to describe these two processes within the frame of collision theory. In I, we studied the excitation of a bulk plasmon by a proton traveling inside aluminum. The excited plasmon eventually decays and a Bloch electron is excited. We considered different lattice contributions to the momentum conservation equation and identified angular and energy regions where most of the electron yield came from plasmon-involved processes (as opposed to binary processes in which the proton interacts directly with a single electron, with no intermediary plasmon). In II, we considered the other process, that is, the excitation of a pair of interacting free electrons as a plasmon decay mechanism. According to our calculations, the two processes together accounted for around 65% of the plasmons excited in aluminum and correctly reproduced the slope of the plasmon excitation curve.

The possibility of a third mechanism by which the plasmon transferred its energy to a single electron and a phonon (phonon-assisted electron excitation) was studied by Sturm and Oliveira [20]. They found that for metals such as Li, Na, and K, this process represented just a minor contribution to the plasmon linewidth. Based on their result, we did not include phonon effects in our calculations.

In this paper, we generalize the results obtained in I and II by considering solids different from aluminum. The theory remains escentially the same although crystal structures will be different along with model potential coefficients, plasmon linewidths, and electron densities. The elements considered are magnesium, sodium, and potassium.

In Sec. II, we summarize the expressions for the differential probability per unit time found in I and II. In Sec. III, graphs are shown for the total probability, excitation power, energy, and angular spectra. Results for aluminum are added in order to establish a comparison. In Sec. IV an approximate scaling rule is found for the $2e$ contributions. Atomic units are used throughout the article.

II. THEORY

The probability per unit time, obtained in I, for a proton and a nearly free (Bloch) electron to interact via the excitation and decay of a bulk plasmon will be referred to as NFe. It reads:

$$\frac{dP^{NFe}}{dt} = 2\pi \int \sum_{\mathbf{G}} \delta(\mathbf{v}_i \cdot \mathbf{p} + \varepsilon_i - \varepsilon_f)\delta(\mathbf{G} - \mathbf{q} + \mathbf{p}) \times \{1 - \Theta[\omega^+(p) - \omega(p)]\Theta[\omega(p) - \omega^-(p)]\} \times 2|T|^2\Theta(k_F - k_i)\Theta(-k_F + k_f)d\mathbf{k}_i d\mathbf{k}_f, \quad (1)$$

where the factor of 2 accounts for spin considerations, $\mathbf{G}$ is the lattice contribution to the momentum conservation equation, $\mathbf{p}$ is the momentum lost by the projectile, the pair $(\omega, \mathbf{q})$ ($\omega = \varepsilon_f - \varepsilon_i = k_f^2/2 - k_i^2/2$ and $\mathbf{q} = \mathbf{k}_f - \mathbf{k}_i$) are the energy and momentum gained by the excited electron, $\mathbf{v}_i$ is the projec-

TABLE I. Crystal structures and lattice parameters [21] are shown for the set Al-Mg-Na-K.

	Al	Mg	Na	K
Crystal structure	fcc	Hexagonal with basis	bcc	bcc
Lattice const. (a.u.)	$a=7.66$	$a=6.05$ $c=9.8$	$a=8.0$	$a=9.9$

tile's initial velocity, k_F is the Fermi momentum and T is the transition matrix, which is given by

$$|T|^2 = |\tilde{V}_P^{eff}(\mathbf{p})|^2 |V_{\mathbf{G}}|^2 \left| \frac{1}{D_i} + \frac{1}{D_f} \right|^2, \tag{2}$$

where $\tilde{V}_P^{eff}(\mathbf{p}) = 4\pi/[(2\pi)^3 p^2 \epsilon_{ML}(p,\omega,\gamma)]$ is the projectile-electron potential in momentum space, $V_{\mathbf{G}}$ is the Fourier transform of the lattice's weak periodic potential, and $D_{i,f} = \varepsilon_{\mathbf{k}_{i,f}} - \varepsilon_{\mathbf{k}_{i,f}\pm\mathbf{G}} + i|V_{\mathbf{G}}|$. Note that $\epsilon_{ML}(p,\omega,\gamma)$ is the Mermin-Lindhard dielectric response with γ the plasmon linewidth at $p=0$.

The probability per unit time, obtained in II, for the projectile to interact with a pair of free interacting electrons, via the excitation and decay of a bulk plasmon will be referred to as $2e$. It reads

$$\begin{aligned} \frac{dP^{2e}}{dt} = 2\pi \int & \delta(\mathbf{v}_i \cdot \mathbf{p} + \varepsilon_{1i} + \varepsilon_{2i} - \varepsilon_{1f} - \varepsilon_{2f}) \\ & \times \delta(-\mathbf{p}_2 - \mathbf{p}_1 + \mathbf{p}) |T|^2 \Theta(k_F - k_{1i}) \\ & \times \Theta(k_F - k_{2i}) \Theta(-k_F + k_{1f}) \Theta(-k_F + k_{2f}) \\ & \times \{1 - \Theta[\omega^+(p) - \omega(p)] \Theta[\omega(p) - \omega^-(p)]\} \\ & \times d\mathbf{k}_{1i} d\mathbf{k}_{1f} d\mathbf{k}_{2i} d\mathbf{k}_{2f}, \end{aligned} \tag{3}$$

with $\mathbf{p}_j = \mathbf{k}_{jf} - \mathbf{k}_{ji}$ the momentum gained by the electron labeled j. In this case, the transition matrix is given by $|T|^2 = \frac{1}{4}|T^S|^2 + \frac{3}{4}|T^A|^2$ and $T^{S/A}$ reads

$$\begin{aligned} T^{S/A} = 2\tilde{V}_P^{eff}(\mathbf{p}) \{ & \tilde{V}_{12}^{eff}(\mathbf{p}_2)[g(\mathbf{k}_i, \mathbf{p}_2) + g(\mathbf{k}_f, -\mathbf{p}_2)] \\ & + \tilde{V}_{12}^{eff}(-\mathbf{p}_1)[g(\mathbf{k}_i, -\mathbf{p}_1) + g(\mathbf{k}_f, \mathbf{p}_1)] \\ & \pm \tilde{V}_{12}^{eff}(\mathbf{k}_{2f} - \mathbf{k}_{1i})[g(\mathbf{k}_i, -\mathbf{k}_{2f} + \mathbf{k}_{1i}) + g(\mathbf{k}_f, -\mathbf{k}_{2f} + \mathbf{k}_{1i})] \\ & \pm \tilde{V}_{12}^{eff}(-\mathbf{k}_{1f} + \mathbf{k}_{2i}) \times [g(\mathbf{k}_i, \mathbf{k}_{1f} - \mathbf{k}_{2i}) + g(\mathbf{k}_f, \mathbf{k}_{1f} - \mathbf{k}_{2i})] \} \end{aligned} \tag{4}$$

where $g(\mathbf{k},\mathbf{q}) = [k^2 - (\mathbf{k}+\mathbf{q})^2 + i0^+]^{-1}$, the effective e-e interaction is $\tilde{V}_{12}^{eff}(\mathbf{q}) = 4\pi Z_{12}/[(2\pi)^3(q^2+\lambda^2)]$ with $\lambda = \sqrt{3}\omega_P/k_F$, and $\mathbf{k} = (\mathbf{k}_2 - \mathbf{k}_1)/2$ is the relative momentum.

III. RESULTS

Our idea is to consider different simple metals and study how their characteristics affect the absolute and relative importance of the plasmon decay mechanisms presented in I and II.

We have worked with the set Al-Mg-Na-K which, on the one hand, includes elements with varied number of valence electrons and different kinds of lattices (see Table I) and, on the other, contains the pair Na-K of alkali metals with the same crystal structure.

TABLE II. Distances to the four nearest neighbors in the reciprocal lattice and model potential coefficients [23] for the elements considered.

	Al	Mg	Na	K
$\lvert\mathbf{G}_1\rvert$ (a.u.)	1.42	1.20	1.11	0.90
$\lvert\mathbf{G}_2\rvert$ (a.u.)	1.64	1.28	1.57	1.27
$\lvert\mathbf{G}_3\rvert$ (a.u.)	2.32	1.36	1.92	1.56
$\lvert\mathbf{G}_4\rvert$ (a.u.)	2.72	1.76	2.22	1.80
$\lvert V_{\mathbf{G}_1}\rvert$ (a.u.)	0.0089	0.0071	0.0103	0.0039
$\lvert V_{\mathbf{G}_2}\rvert$ (a.u.)	0.0281	0.0133	0.0046	0.0027
$\lvert V_{\mathbf{G}_3}\rvert$ (a.u.)	0.0272	0.0186	0.0018	0.0077
$\lvert V_{\mathbf{G}_4}\rvert$ (a.u.)	0.0093	0.0215	0.0035	0.0115

Starting with plasmon decay via the excitation of a Bloch electron (NFe, studied in I), the lattice contribution to the momentum conservation equation is given by the points $\mathbf{G}_i$ in momentum space which determine the reciprocal lattice. The distances $|\mathbf{G}_i|$, $1 \leqslant i \leqslant 4$, to the four nearest neighbors (displayed in Table II) were used to calculate the model potential coefficients $V_{\mathbf{G}_i}$, $1 \leqslant i \leqslant 4$, where the physics of the electron-lattice interaction is condensed [22,23].

When it comes to plasmon decay via the excitation of two interacting free electrons ($2e$, studied in II), the crystal structure is irrelevant and it is the electron densities we want to compare.

Finally, both processes will be influenced by the value of the plasmon linewidth [16,24–26] whose experimentally determined values at $p=0$ are shown in Table III together with other illustrative information.

In Fig. 1, the probabilities of plasmon decay per unit time are shown together with the plasmon excitation curves. The general curve shapes for the four elements are very similar and, as expected, larger electron densities favor plasmon excitation. Also, the threshold velocities (minimum velocity required to excite a plasmon) are different, becoming lower for lower electron densities.

Looking at the NFe curves it is interesting to observe that this mechanism is negligible for potassium. We can understand this result if we compare potassium's model potential coefficients with those of sodium, magnesium, or aluminum. Those of potassium are no more than 1/3 of those for the

TABLE III. Electron densities [21] for the elements considered, together with plasmon linewidths [16,24–26] and other illustrative information.

	Al	Mg	Na	K
η (density) (a.u.)	0.0254	0.0129	0.004	0.002
k_{Fer} (a.u.)	0.9094	0.7256	0.487	0.390
ω_p (a.u.)	0.56	0.40	0.22	0.16
γ (plasmon linewidth) (a.u.)	0.037	0.051	0.009	0.009

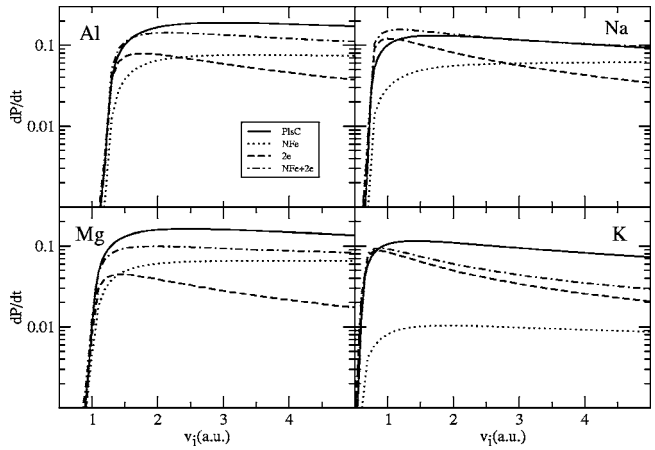

FIG. 1. The probabilities per unit time are displayed for Al-Mg-Na-K. Plasmon excitation (PlsC) is shown with a solid line. Plasmon excitation and later decay by the excitation of a Bloch electron (NFe) is shown with a dashed line. Plasmon excitation and later decay via the excitation of two interacting free electrons ($2e$) is shown with a dot-dashed line. The dot-double-dashed line stands for NFe+$2e$.

other elements as its electrons are, in real space, relatively farther from the ion lattice. In addition, results for all the elements confirm that a larger electron density helps the NFe mechanism.

Graphs for magnesium and aluminum behave alike. At v_i=5 a.u., NFe+$2e$ accounts for around 62% of the excited plasmons in magnesium and around 65% in aluminum. Also the $2e$ mechanism is more important in aluminum due to its higher electron density.

Now, as we turn our attention to sodium, we find that, at low projectile velocities, there are more decaying plasmons than excited ones. We cannot find an explanation for this in the model. We think it might be related to the plasmon linewidth value which could be not as accurate as the ones for aluminum and magnesium. Actually, when looking at aluminum or potassium, one sees some overestimation at low velocities but not nearly as important as that found in sodium.

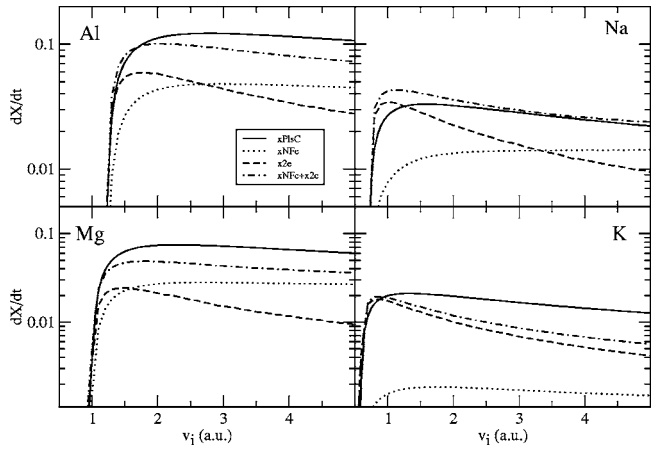

FIG. 2. The excitation powers per unit time are displayed for Al-Mg-Na-K. Line types represent the same processes they did in Fig. 1.

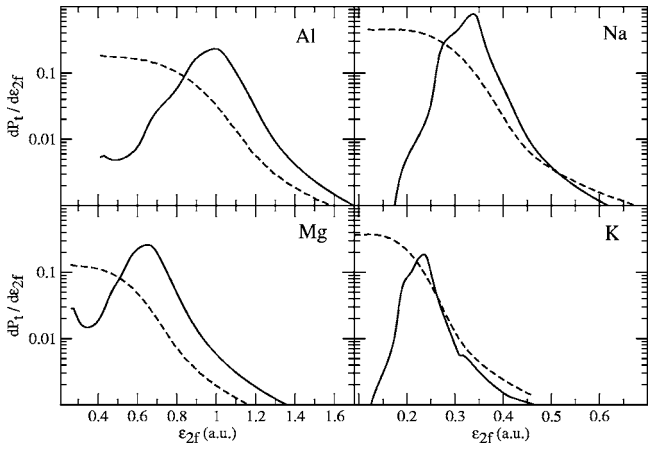

FIG. 3. The first-differential energy spectra are shown for Al-Mg-Na-K at v_i=2 a.u. The solid line stands for the NFe contribution while the dashed line stands for the $2e$ one. Energies are measured from the bottom of the band.

In Fig. 2, the excitation powers ($dX=\omega\, dP$) per unit time for plasmon decay are shown together with the stopping power curves. We encounter the same qualitative characteristics found for the probabilities.

In Fig. 3, first-differential energy spectra are shown, at v_i=2 a.u., for the two mechanisms and the four elements. The NFe curves show a peak at $\varepsilon_f=\varepsilon_i+\omega_p$. In addition, at the left of the main peak, we find similar structures for every element, though less pronounced in magnesium, the only one without a cubic crystal structure. Also, in potassium, we find a structure to the right of the peak that is not present for the other elements. We do not know what this structure might be related to.

As for the $2e$ contributions to the spectra, the shapes of the curves are alike for all the elements but we find it puzzling that sodium or potassium (both with only one valence electron per atom) present, at $\varepsilon_{2f}=\varepsilon_{Fer}$, larger values than magnesium or aluminum (two and three valence electrons per atom, respectively).

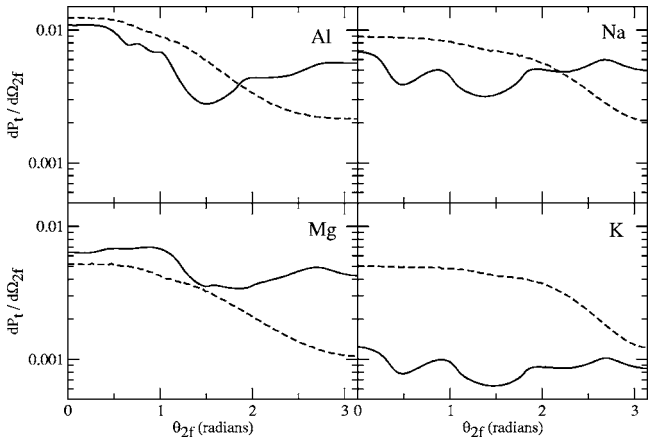

FIG. 4. The first differential angular spectra are shown for Al-Mg-Na-K at v_i=2 a.u. The solid line stands for the NFe contribution while the dashed line stands for the $2e$ one. Angles are referred to the projectile's initial velocity.

In Figure 4, first-differential angular spectra are shown, at $v_i=2$ a.u., for the two mechanisms and the four elements. It is interesting to observe that, for NFe in sodium and potassium (both bcc), the curve structure is exactly the same. If we were working with monocrystals, this result might not come as a surprise. The reciprocal lattice's geometry favors certain directions for the excitation of the Bloch electron. However, we are actually dealing with polycrystals where the orientation of the crystal is randomly changed as the projectile travels inside it. We find that despite this, some memory of the crystal geometry persists. Also we mention the fact that the three cubic elements (Al, Na, and K) present a well in the normal direction (with respect to the projectile's velocity).

Finally, the $2e$ angular spectra are qualitatively similar for all the elements, with most of the excited electrons moving in the forward direction. Oddly, sodium and potassium have $2e$ contributions that are more important than those of magnesium.

IV. SCALING RULES

A. Scaling for the plasmon creation probability and stopping power

The probability for a projectile with charge Z_P and velocity v_i to transfer momentum p and energy ω to the free-electron gas (FEG) is well known from the literature [27] and reads

$$P(p,\omega,\gamma) = -\frac{2Z_P^2}{\pi v_i}\frac{1}{p}\mathrm{Im}\left(\frac{1}{\epsilon(p,\omega,\gamma)}\right). \tag{5}$$

Therefore, the total transition probability is

$$\frac{dP}{dt} = \int_0^{2v_i} dp \int_0^{+\infty} d\omega\, \Theta(p-\omega/v_i) P(p,\omega,\gamma), \tag{6}$$

where we have considered $\epsilon(p,\omega,\gamma)$ to be Mermin-Lindhard's dielectric response which includes the possibility of both binary and plasmon excitations in the mentioned FEG ($dP=dP^{bin}+dP^{pls}$). The plasmon linewidth γ associated with the damping of collective excitations is a rather irrelevant parameter unless one is interested in what happens to plasmons after they are excited. In fact, Eq. (6) is practically insensitive to changes in γ and, for a given projectile, depends only on k_F.

It can be easily shown that, when considering only collective excitations, Eq. (6) is approximately proportional to $\sqrt{k_F}$ [27] (neglecting an extra logarithmic dependence), and therefore, the plot $(dP^{pls}/dt)k_F^{-1/2}$ vs v_i/k_F will be, also approximately, *element independent* as is shown in Fig. 5(a) for the elements considered in this article ($0.39<k_F<0.91$).

Analogous results can be found for the stopping power S which reads

$$\frac{dS}{dt} = \int_0^{2v_i} dp \int_0^{+\infty} \omega\, d\omega\, \Theta(p-\omega/v_i) P(p,\omega,\gamma). \tag{7}$$

In this case, as $dS^{pls}/dP^{pls}\sim\omega_P\sim k_F^{3/2}$, the approximate proportionality is to k_F^2 and therefore, the plot $(dS^{pls}/dt)k_F^{-2}$ vs v_i/k_F will be, also approximately, *element independent* [see Fig. 5(b)].

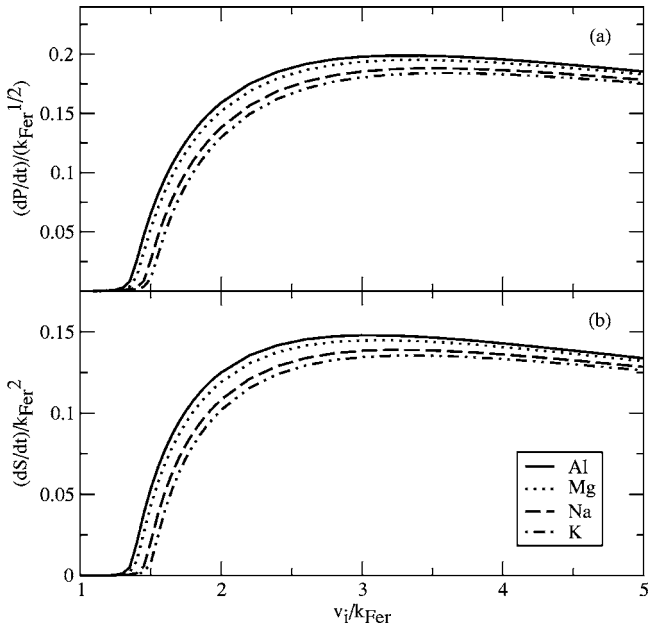

FIG. 5. Scaling rule for the plasmon creation probability and stopping power.

B. Scaling for the $2e$ contribution to plasmon decay

The results obtained in the previous subsection suggest the idea of finding a similar scaling rule for the $2e$ contribution to the plasmon decay probability dP^{2e}/dt, given by Eq. (3). It is important to remark that results for dP^{2e}/dt depend on two mutually independent gas parameters: k_F and γ. The scaling will be possible if we can factor out these parameters by performing some changes of variables.

We start by referring every momentum to k_F, that is, we define new variables $k'=k/k_F$. This allows the function $g(\mathbf{k},\mathbf{q})$ in Eq. (4) to be expressed as $g(\mathbf{k}',\mathbf{q}')/k_F^2$. However, when we turn to the potential $\tilde{V}_{12}^{eff}(\mathbf{q})$, we find that it cannot be "k_F cleaned" exactly because $\lambda=\sqrt{3}\omega_P/k_F=2\sqrt{k_F}/\sqrt{\pi}$ does not scale as a momentum.

Furthermore, the potential $\tilde{V}_P^{eff}(\mathbf{p})$ does not scale either due to the lack of scaling properties of $\epsilon(p,\omega,\gamma)$. Regarding the dielectric response, note that it is the only part of dP^{2e}/dt that actually depends on γ. Also, it is important to mention that the main contribution to $\mathrm{Im}[1/\epsilon(p,\omega,\gamma)]$ for zero-momentum plasmons comes from $\omega\sim\omega_P$ which scales with $k_F^{3/2}$, but, inside the binary region, this scaling changes and ω approximately scales with k_F^2.

Despite all these complications, we managed to obtain an approximate scaling rule proceeding as follows. First, ficticious aluminumlike elements Mg^*, Na^*, and K^* were defined, their plasmon linewidths γ^* satisfying

$$\frac{\gamma^{\mathrm{Al}}}{(k_F^{\mathrm{Al}})^2} = \frac{(\gamma^*)^B}{(k_F^B)^2}, \tag{8}$$

with $B=$Al, Mg, Na, K. Letting dP_B^{*2e}/dt and dX_B^{*2e}/dt be the probability and excitation power for these pseudoelements,

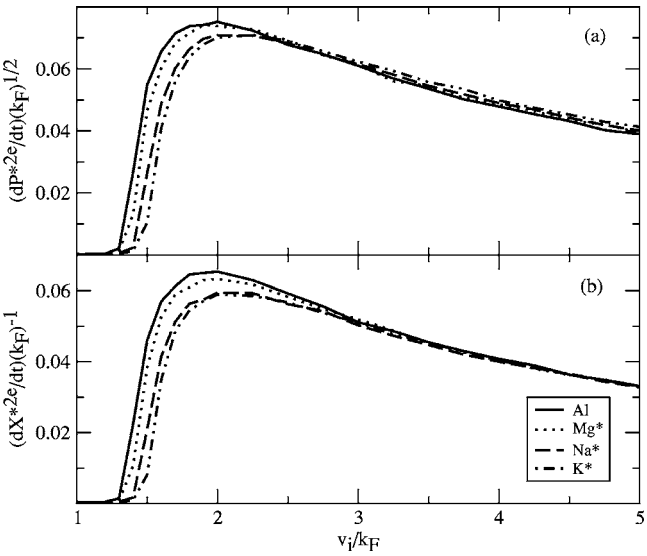

FIG. 6. Approximate scaling rule for the $2e$ contribution to the plasmon decay probability and excitation power. Note that, for an element B, dP^{*2e}/dt and dX^{*2e}/dt are related to dP^{2e}/dt and dX^{2e}/dt (results for the real elements), as indicated by Eq. (9), that is, $dP^{2e}/dt=(\gamma^{\mathrm{Al}}/\gamma^{B})^{0.9}(k_F^B/k_F^{\mathrm{Al}})^{1.8}(dP^{*2e}/dt)$ and $dX^{2e}/dt=(\gamma^{\mathrm{Al}}/\gamma^{B})^{0.9}(k_F^B/k_F^{\mathrm{Al}})^{1.8}(dX^{*2e}/dt)$.

we found that the plots $(dP_B^{*2e}/dt)\sqrt{k_F^B}$ vs v_i/k_F^B and $(dX_B^{*2e}/dt)/k_F^B$ vs v_i/k_F^B were approximately element independent (note that $dX^{2e}/dP^{2e}\sim\omega_P\sim k_F^{3/2}$). These results are shown in Fig. 6 where it can be observed that these rules are almost exact for high values of v_i/k_F.

Second, an empirical rule was found that relates the probabilities and excitation powers associated with the real elements, dP_B^{2e}/dt and dX_B^{2e}/dt, with those associated with the aluminumlike elements, dP_B^{*2e}/dt and dX_B^{*2e}/dt. This rule reads

$$\frac{dP_B^{2e}}{dt}\cong\frac{dP_B^{*2e}}{dt}\left(\frac{\gamma^{*B}}{\gamma^{B}}\right)^{0.9},$$

$$\frac{dX_B^{2e}}{dt}\cong\frac{dX_B^{*2e}}{dt}\left(\frac{\gamma^{*B}}{\gamma^{B}}\right)^{0.9}, \tag{9}$$

and combining these relations with Eq. (8) we get

$$\frac{dP_B^{2e}}{dt}\cong\frac{dP_B^{*2e}}{dt}\left(\frac{\gamma^{\mathrm{Al}}}{\gamma^{B}}\right)^{0.9}\left(\frac{k_F^B}{k_F^{Al}}\right)^{1.8},$$

$$\frac{dX_B^{2e}}{dt}\cong\frac{dX_B^{*2e}}{dt}\left(\frac{\gamma^{\mathrm{Al}}}{\gamma^{B}}\right)^{0.9}\left(\frac{k_F^B}{k_F^{Al}}\right)^{1.8}. \tag{10}$$

These last expressions, together with the results displayed in Fig. 6, provide a reasonable scaling which should be useful for estimating dP^{2e}/dt and dX^{2e}/dt for an arbitrary metal in terms of its parameters k_F,γ and the references $k_F^{\mathrm{Al}},\gamma^{\mathrm{Al}}$.

V. SUMMARY AND CONCLUSIONS

In this paper, we applied the models for projectile-induced plasmon excitation and decay, developed in I and II for aluminum, to other simple metals.

The results obtained for the NFe mechanism could be understood in terms of the different crystal structures despite the fact that we were working with polycrystals. Also, we found that this mechanism is negligible in potassium as its electrons are farther from the heavy but screened nuclei. In both the energy and angular spectra we found similarities between Al, Na, and K that, we think, are due to the common cubic structure (fcc or bcc).

The results obtained for $2e$ depended only on the electronic density and the plasmon linewidth. The curve shapes were similar for all the elements considered but some overestimation at low velocities was found for the case of sodium. We could not explain this and we tend to think it might be related to the plasmon linewidth which might not be as accurate as the ones used for aluminum and magnesium.

Total results for magnesium were particularly reliable, accounting for 62% of the excited plasmons at high velocities, very similar to the 65% explained in aluminum.

We were able to verify the well-known scaling rule for both the plasmon creation probability and stopping power. Also, an approximate scaling rule was found for the $2e$ contribution to the plasmon decay probability and excitation power.

It is important to mention that we restricted ourselves to the use of the simplest dielectric function that includes plasmon damping, that is, Mermin-Lindhard's. Our results could be refined by means of a more elaborated dielectric response.

ACKNOWLEDGMENTS

This work was done with the financial support of UBA-CyT, CONICET, and ANPCyT.

[1] C. Benazeth, N Benazeth, and L. Viel, Surf. Sci. **78**, 625 (1978).
[2] D. HasselKamp and A. Scharmann, Surf. Sci. **119**, L388 (1982).
[3] M. F. Burkhard, H. Rothard, and K.-O. E. Groeneveld, Phys. Status Solidi B **147**, 589 (1988).
[4] A. A. Almulhem and M. D. Girardeau, Surf. Sci. **210**, 138 (1989).
[5] E. A. Sánchez, J. E. Gayone, M. L. Martiarena, O. Grizzi, and R. A. Baragiola, Phys. Rev. B **61**, 14209 (2000).
[6] R. Zimmy, Surf. Sci. **260**, 347 (1992).
[7] N. J. Zheng and C. Rau, J. Vac. Sci. Technol. A **11**, 2095 (1993).
[8] R. A. Baragiola and C. A. Dukes, Phys. Rev. Lett. **76**, 2547

(1996).
[9] S. M. Ritzau, R. A. Baragiola, and R. C. Monreal, Phys. Rev. B **59**, 15506 (1999).
[10] N. Stolterfoht, D. Niemann, V. Hoffmann, M. Rösler, and R. Baragiola, Phys. Rev. A **61**, 052902 (2000).
[11] P. Riccardi, P. Barone, A. Bonanno, A. Oliva, and R. A. Baragiola, Phys. Rev. Lett. **84**, 378 (2000).
[12] S. Lacombe, V. A. Esaulov, E. A. Sánchez, O. Grizzi, and N. R. Arista, Phys. Rev. B **67**, 125418 (2003).
[13] P. Nozières and D. Pines, Phys. Rev. **113**, 1254 (1969).
[14] M. Rösler and W. Brauer, Phys. Status Solidi B **104**, 161 (1981).
[15] M. Rösler and W. Brauer, *Particle Induced Electron Emission I*, Springer Tracts in Modern Physics Vol. 122 (Springer, Berlin, 1991), p. 1.
[16] M. Rösler, Appl. Phys. A: Mater. Sci. Process. **61**, 595 (1995).
[17] D. F. DuBois, Ann. Phys. (N.Y.) **8**, 24 (1959).
[18] G. Bocan and J. E. Miraglia, Phys. Rev. A **67**, 032902 (2003).
[19] G. A. Bocan and J. E. Miraglia, Phys. Rev. A **69**, 012901 (2004).
[20] K. Sturm and L. E. Oliveira, Phys. Rev. B **24**, 3054 (1981).
[21] N. W. Ashcroft and N. D. Mermin, *Solid State Physics* (Holt, New York, 1976).
[22] A. O. E. Animalu and V. Heine, Philos. Mag. **12**, 1249 (1965).
[23] W. A. Harrison, *Pseudopotentials in the Theory of Metals* (W. A. Benjamin, New York, 1966).
[24] N. R. Arista, Phys. Rev. A **49**, 1885 (1994).
[25] I. Abril, R. García-Molina, C. D. Denton, F. J. Pérez-Pérez, and N. R. Arista, Phys. Rev. A **58**, 357 (1998).
[26] P. C. Gibbons, Phys. Rev. B **17**, 549 (1978).
[27] D. Pines and D. Bohm, Phys. Rev. **85**, 338 (1952).